Photochemical & Photobiological Sciences (2023) 22:2781–2798
https://doi.org/10.1007/s43630-023-00486-2

ORIGINAL PAPERS

Application of molecular dynamic simulations in modeling the excited state behavior of confined molecules

Dipendra Khadka[1] · Vindi M. Jayasinghe-Arachchige[1] · Rajeev Prabhakar[1] · Vaidhyanathan Ramamurthy[1]

Received: 27 June 2023 / Accepted: 20 September 2023 / Published online: 16 October 2023

Abstract

Relative to isotropic organic solvent medium, the structure and conformation of a reactant molecule in an organized and confining medium are often different. In addition, because of the rigidity of the immediate environment, the reacting molecule have a little freedom to undergo large changes even upon gaining energy or modifications in the electronic structure. These alterations give rise to differences in the photochemistry of a molecular and supramolecular species. In this study, one such example is presented. α-Alkyl dibenzylketones upon excitation in isotropic solvents give products via Norrish type I and type II reactions that are independent of the chain length of the alkyl substituent. On the other hand, when these molecules are enclosed within an organic capsule of volume ~ 550 $Å^3$, they give products that are strikingly dependent on the length of the α-alkyl substitution. These previously reported experimental observations are rationalized based on the structures generated by molecular modeling (docking and molecular dynamics (MD) simulations). It is shown that MD simulations that are utilized extensively in biologically important macromolecules can also be useful to understand the excited state behavior of reactive molecules that are part of supramolecular assemblies. These simulations can provide structural information of the reactant molecule and the surroundings complementing that with the one obtained from 1 and 2D NMR experiments. MD simulated structures of seven α-alkyl dibenzylketones encapsulated within the octa acid capsule provide a clear understanding of their unique behavior in this restricted medium. Because of the rigidity of the medium, these structures although generated in the ground state can rationalize the photochemical behavior of the molecules in the excited state.

Graphical abstract

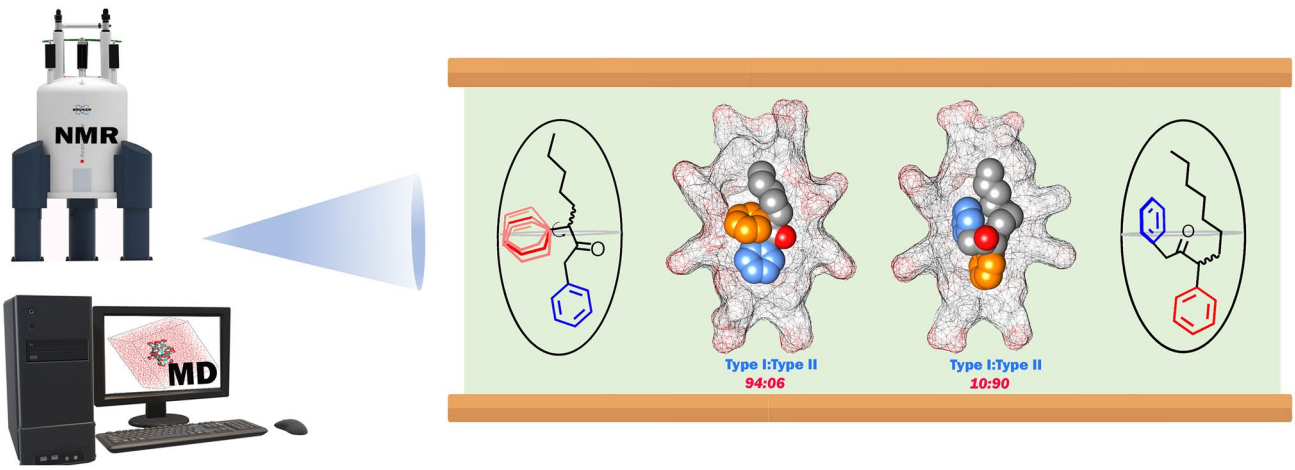

Keywords Supramolecular photochemistry · Confinement · Molecular dynamics simulation · Norrish type I and type II reaction · α-alkyl dibenzylketones

Extended author information available on the last page of the article

1 Introduction

Molecular organic photochemistry concerns with predicting and understanding the behavior of electronically excited molecules in isotropic solution and in gas phase [1, 2]. In these media, photochemical transformations are understood on the basis of the assumption that following vertical excitation, the new electronic configuration controls the nuclei motion. In the absence of strong intermolecular interactions, the environment has a little influence on these dynamics. Examination of several organic molecules in isotropic solution has led photochemists to recognize that a better control of molecular behavior on the excited state surface can be achieved in a highly organized and confining environment, where the mobilities of the nuclei are restricted and changes in the electronic configuration will not have much influence on the positions of nuclei [3–6]. Such environments include crystals, zeolites, and rigid host – guest complexes in solution. In a 'hard' medium, in contrast to an isotropic solvent, the new electronic configuration generated by excitation of a guest molecule will not be able to easily influence the nuclei positions [7, 8]. Therefore, under these conditions, the excited state chemistry would be controlled essentially by the ground state structure of molecules. The best example of this is the photoreactions in the crystalline state [9–11]. The fact that photoreactions in crystalline state can be rationalized on the basis of the 'reaction cavity concept' and 'topochemical postulate' developed by Schmidt, Cohen, and coworkers by correlating the crystal structures with reactivities to understand the photoreactions in the crystalline state is a clear example of ground state nuclear structure controlling the excited state chemistry [9, 12–14]. The above condition can also occur in solution to provide the medium in which the reaction occur is hard and inflexible [7, 8]. This study represents one such supramolecular assembly in aqueous solution, namely, an organic capsule solubilized in water where the walls are rigid and inflexible similar to that in crystals. The reaction cavity we are concerned with is a capsule made of two molecules of octa acid (OA, **1**) [15]. The structure, chemical formula and the internal dimensions of OA capsule are shown in Fig. 1. In these capsules, we believe like crystals the excited state reactivity of the included guest will be controlled by the ground state structure of the reactant. Also, it is important to recognize that the structure inferred in isotropic solution may not be helpful to understand the excited state behavior within the capsule. Thus, knowing the ground state structure of guest molecules in these rigid capsules is sufficient to understand their excited state behavior.

Unlike typical organic molecules, since supramolecular complexes do not readily crystallize, one needs reliable methods that can identify the structure of the reactant in the complex. One of the commonly used experimental tools in supramolecular chemistry is ^{1}H NMR spectroscopy. With increasing applications of molecular dynamics (MD) simulations in predicting the structures of small and large molecules, we explored its applicability in qualitatively predicting photoreactions of molecules within OA capsule [16–18]. The information obtained from MD simulations can complement (and in some cases substitute) the information gleaned from the ^{1}H NMR spectroscopy. These simulations have been extensively used in biological systems to study protein – protein, protein – drug, and enzyme – substrate interactions [19–26]. It needs to be emphasized that in these simulations, the electronic effects of molecules are ignored, and the host – guest complexation is promoted by noncovalent interactions, such as Van der Waals and electrostatic interactions [27–29]. Despite these limitations, [30, 31] elucidations of the structures and dynamics of molecules in the confined medium by these simulations would be useful to understand photoreactions.

The aim of this study is to examine the value of MD simulations to rationalize reactivity of molecules in the OA capsule. Like X-ray crystal structures that help foresee the reactivity of molecules in the crystalline state, we anticipate that the structures deduced by MD simulations would be valuable to predict photoreactions of molecules in restricted spaces. With this goal, we proceeded to examine the MD simulations of an experimentally well-investigated system, α-alkyl dibenzylketones (**2a – h**) within a closed organic capsule of octa acid (OA, **1** Fig. 1) [15, 32]. The structures of α-alkyl dibenzylketones **2a – h**, reactions and products are provided in Scheme 1. In a previous study, we established through ^{1}H NMR titrations that these molecules form 2:1 (host:guest) complexes [32]. For a detailed discussion, the readers are referred to the earlier publication. The DBK molecules **2c – h** upon excitation in an organic solvent undergo both Norrish type I and type II reactions; ketones **2a – b** due to the lack of γ-hydrogens react only via Norrish type I (Scheme 1). In isotropic solution, the products AA, AB, and BB (**3 – 8**) resulting from Norrish type I and cyclobutanol **11** and olefin **13** from Norrish type II reaction (Scheme 1) were independent of the length of the alkyl chain (Table 1). On the other hand, within the OA capsule, although the primary photoreactions are the same as in organic solvent (Norrish type I and type II reactions), the products and their distributions are different. In addition, they depend on the length of the alkyl chain (Table 1). Earlier, the alkyl chain length dependent products distributions was rationalized utilizing the structures of DBK **2a – h** within the OA capsule derived from 1 and 2D NMR spectra (Fig. 2) [32]. This is an elegant example where the 'new' electronic configuration (excited state) and 'original'

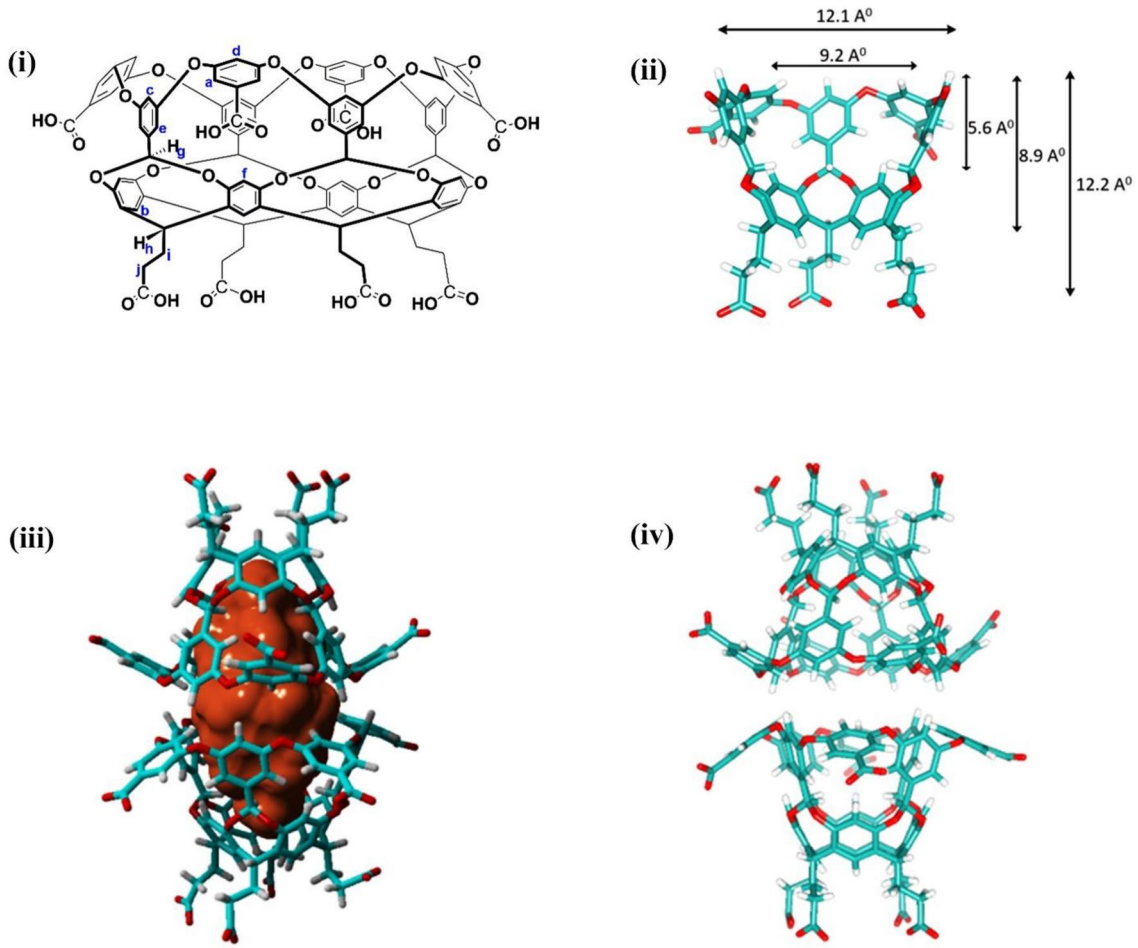

Fig. 1 Chemical structure of the host octa acid, **1** (OA), its internal dimensions and capsular assembly of two molecules of OA showing the internal space (red filling). The labels a – j in chemical structure of OA (i) represents distinct identifiable proton signals in NMR

nuclear configuration (ground state) control the reactivity. In this study, the same set of molecules was used as a test case to validate the applicability of MD simulated structures in exploring structure – reactivity relationships in confined spaces. The results presented here suggest that MD simulations can be used as a complementary or additional tool to predict and understand photoreactions of α-alkyl dibenzylketones **2a – h** within the OA capsule. In fact, it provides additional information on interatomic distances that are not accessible through 1-D NMR spectroscopy. This opens a possibility of predicting the reactivity of molecules enclosed in small spaces based on the MD simulated structures. It is worth mentioning that MD simulations are not guaranteed to provide accurate structures that are supported by the measured NMR data. A guest molecule can adopt many different conformations inside the cavity of a host molecule and will need optimum conditions to find the global minimum. Thus, a successful outcome of these simulations depends on the quality of initial structures, sufficient time lengths, and accurate modeling of experimental conditions.

Although considering the usefulness of MD simulations in generating structures of host–guest complexes it is important to highlight their advantages and limitations. These simulations can provide a link between structure, reactivity, and dynamics by enabling the exploration of the conformational energy landscape accessible to both host and guest molecules. Quite remarkably, even short timescale MD simulations can reproduce many experimental parameters. However, their accuracies depend on the precise simulations of molecular structures and experimental conditions, such as solvent, temperature, and pH. The quantum mechanical methods can accurately model geometrical parameters, such as bond lengths, angles, and dihedrals of many molecules [33]. However, these are restricted to relatively small molecules even with the supercomputing power available these days. The multiscale approaches, such as hybrid quantum

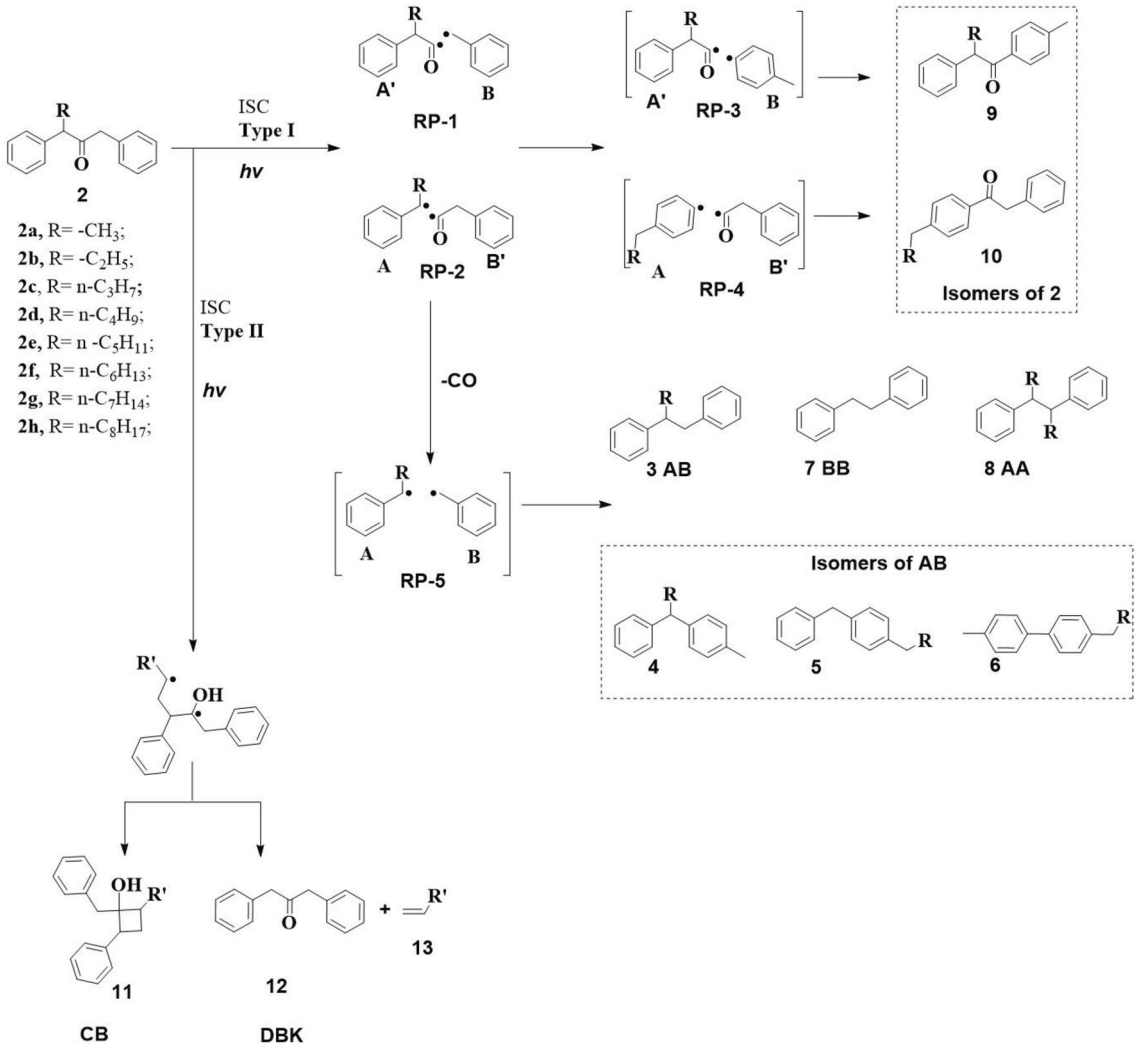

Scheme 1 Photoreactions and products upon excitation of α-alkyl dibenzylketones **2a – h**

Table 1 Products formed upon photolysis of α-alkyldibenzyl ketones in hexane.[a]

Reactant α-alkyl DBK	Type I products					Type II products		Type I: Type II products
	AA (**8**)	AB (**3**)	BB (**7**)	(**9**)	(**10**)	DBK (**12**)	CB (**11**)	
2a	24	48	28	0	0	–	–	–
2b	23	48	29	0	0	–	–	–
2c	16	40	24	0	0	11	9	80:20
2d	17	45	20	0	0	7	11	82:18
2e	16	41	23	0	0	4	16	80:20
2f	15	46	32	0	0	4	3	93:7
2 g	13	49	26	0	0	4	8	88:12
2 h	16	46	23	0	0	5	10	85:15

[a]Structures of, **2, 3**, **7**–**12**, DBK, and CB are included in Scheme 1. The data taken from Ref. 32

mechanics/molecular mechanics (QM/MM) methods can provide an accurate treatment of large macromolecules [33–35]. In these methods, the electronic effects of atoms in the QM layer are included and electrostatic and steric effects of the atoms in the MM layer are incorporated.

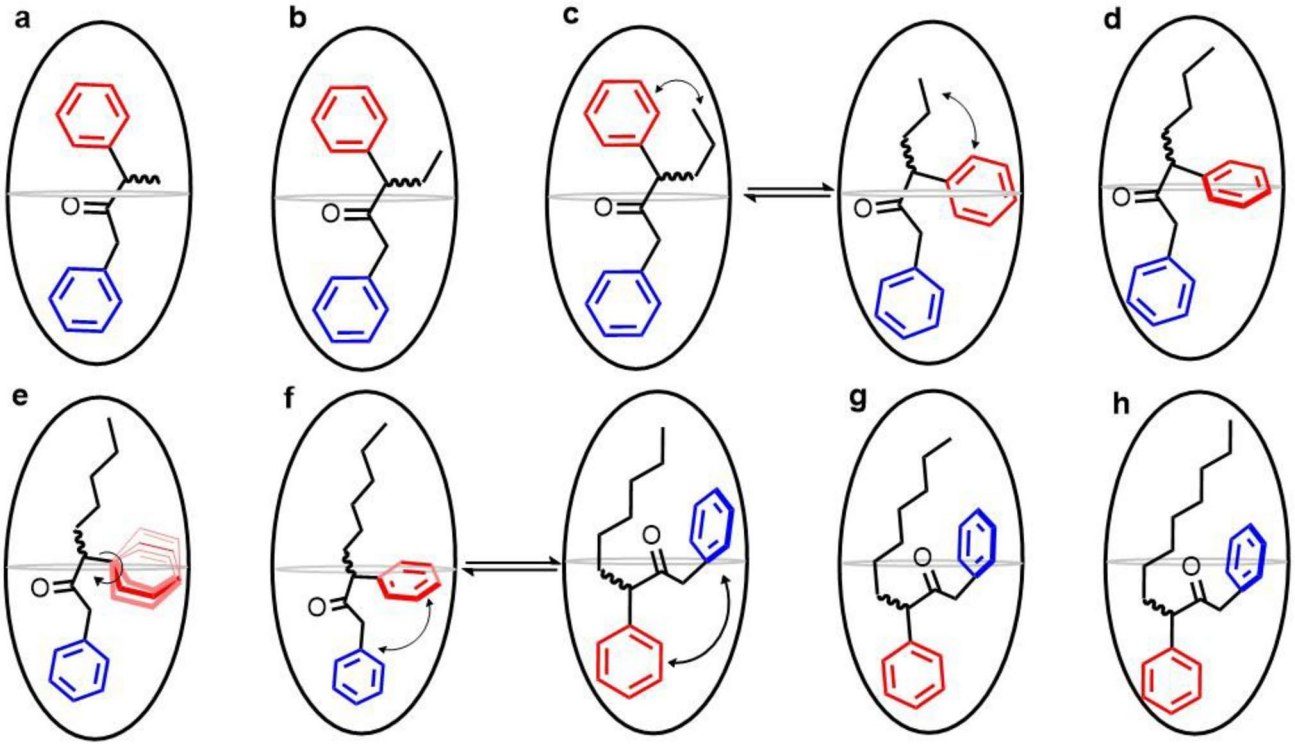

Fig. 2 Conformations of octa acid encapsulated α-alkyldibenzyl ketones as inferred from ^{1}H NMR spectra. The double headed arrows in **c** and **f** indicate the possible existence of two conformations in equilibrium within octa acid. The figure was adopted from ref. 32

However, these methods are not straight forward to use and include several considerations such as choice of right DFT functionals, basis set, electrostatic embedding, treatment of QM – MM interphase, etc. that require special expertise and powerful computational resources. In addition, QM/MM optimizations are driven by the maximization of chemical interactions for the minimization of energy and do not include the effects of molecular dynamics. On the other hand, the QM/MM MD simulations that include dynamics can be run for a very short time (a few hundred picoseconds) and may not provide very meaningful structures. Therefore, these types of simulations are often performed using semi-empirical methods [36–44]. In comparison to these sophisticated methods, MD simulations are simpler and easier to run for nonexperts with modest computational resources. They rely on the quality of force field (FF) parameters to mimic structural properties of molecules and can be applied to much larger molecules, especially host – guest complexes. Quite clearly, a single computational method cannot address all chemical issues. Based on the nature of a chemical problem, a suitable method needs to be selected. In the last decade, there has been a marked improvement in quality of these parameters and several FFs have been developed [45–48]. They perform quite well in modeling standard (well-known) molecules. However, extra caution is needed while simulating nonstandard (relatively unknown) molecules using these FFs. As discussed below, MD simulations identify conformations for all eight ketones (**2a – h**) that are the same as the ones inferred from NMR (Fig. 2). In addition, information regarding interatomic interactions and available free space within the capsule that help to rationalize products preference, not available from NMR, is also revealed. The results presented here validate the applicability of MD simulations in obtaining the structures of reactant molecules within a confined space and enable interpretation of the excited state behavior of an entrapped molecule.

2 Computational Methods

The OA (host) and DBK (guest) simulations were performed using the following multi-step procedure.

Structures of host and guest molecules: The guest molecules, DBK **2a – h**, were modeled using the Gauss View 5.0 program, and the 3D structure of OA was obtained from our previous study [49]. These structures were optimized without any geometrical constraints at the B3LYP [50, 51]/GD3BJ [52] level of theory utilizing the Gaussian 09 software package [53]. In these calculations, the O atoms were treated with 6 – 31 + g(d) and C and H with the 6 – 31 g(d) basis set, respectively [54, 55]. The effects of the surrounding solvent environment were incorporated

using a dielectric constant of 2.3, corresponding to benzene, and utilizing the self-consistent reaction field (SCRF) integral equation formalism polarizable continuum model (IEFPCM) method [56].

Calculations of Charges: The restrained electrostatic potential (RESP) atomic charges for the OA and guest molecules were calculated using antechamber [57, 58], an inbuilt tool in the Amber program [59]. These charges were utilized to create topology files that define molecular parameters.

Starting structures of host – guest complexes: The initial structures of host – guest complexes were built using molecular docking performed utilizing the Auto Dock Vina 1.5.6 program package [60]. In this procedure, different conformations of the guest were used to identify the potential biding sites within the entire cavity of the host. Based on their binding energies, multiple poses of host – guest complexes for each guest molecule were obtained.

Molecular Dynamics (MD) simulations: The most promising poses provided by the previous docking procedure were subsequently used for MD simulations utilizing the GROMACS [61, 62] program package and AMBER03 [63] force field. In all simulations, the starting structure (host – guest complex) was placed in a cubic box with dimensions of $60 \times 60 \times 60$ Å^3, and the remaining space of the box was filled with the TIP3P water molecules [64]. Then, the system was neutralized by replacing some water molecules with sodium and chloride ions. These models were subsequently energy-minimized with a steepest descent method for 3000 steps. All MD simulations were performed on the energy-minimized structures for 100 ns using a constant number of particles (N), pressure (P), and temperature (T) (NPT ensemble). The bond lengths of the OA were constrained by the LINCS [65] algorithm whereas the SETTLE [66] algorithm was used to constrain the bond lengths and angles of the water molecules. The long-range electrostatic interactions were calculated by the Particle-Mesh Ewald method [67]. The MD trajectories for each model were calculated with a time step of 2 fs. Next, the most representative structures for the OA – guest complexes were derived from a cluster analysis. The analysis of the root-mean-square deviations (RMSDs) along the trajectories showed that structures were well equilibrated within the simulation time. In addition, simulations for the **2a**, **2c**, **2d**, and **2e** were repeated at 500 K to explore the behavior of these complexes at a higher temperature. An increase in temperature will test the stability of a specific conformation by providing the system enough energy to explore other conformations on the energy surface. In addition, in some cases, simulation time was extended to 200 ns to validate the stability of the complexes formed.

Binding energy and single point energy calculations: The binding energy of guests within the host pocket was calculated using the Molecular Mechanics Poisson–Boltzmann Surface Area (MM-PBSA) method [68] and a relevant comparison was made to find the best favorable conformation for each complex. The absolute value of this FF-based binding energy is not meaningful, but the difference in its values for two conformers can be used to identify the most plausible binding mode of a guest inside the cavity of OA. A high value of binding energy doesn't represent the thermodynamic stability of a host – guest complex. A guest with a high binding energy can distort the structure of the OA capsule and increase the overall energy of the host – guest complex. The most representative host – guest complexes obtained from MD simulations were subjected to single-point energy calculations at the quantum mechanical level (B3LYP/6–31 + g(d)) using the Gaussian 09 program package. These calculations will provide their electronic energies that cannot be computed using molecular mechanics-based methods. These pure QM energies of the different conformers of the host – guest complexes are compared to determine the most stable host – guest structure. These energies are not applied to the potentials used in MD simulations. Recently, the binding energies computed using QM/MM approaches were reported to be similar to those calculated with MM methods for the octa-acid host.[40].

Distance between γ-H and carbonyl oxygen atom: The 100 ns MD simulation trajectories were used in the visual molecular dynamics [69] (VMD) software to compute the average distance between the γ-H and carbonyl oxygen atom. This distance is critical for the type II Norrish reaction. If more than one equilibrated conformation was provided by MD simulations, this distance was used as an additional parameter to determine the preferred structure.

Additional Analysis and Visualization: The volume of the OA cavity after removing DBK **2a – h** from the complex was calculated using a plugin in Yasara 13.2.2 package [70] For visualization and preparation of the structural diagrams, Yasara, Chimera[71], and VMD programs were utilized.

3 Results

A closer look at Table 2 reveals that the ketones **2a – h** based on their photochemical behavior within the OA capsule could be divided into three groups—(1): undergoes mainly Norrish type I reaction giving the coupling product **AB** and the rearranged ketone **10** as the main product (**2a**, **2b,** and **2c**); (2): undergoes mainly Norrish type I reaction giving **AB** and the rearranged ketones **9** and **10** as products (**2d** and **2e**) and (3): undergoes both Norrish type I and type II reactions and the latter predominates as the chain gets longer

Table 2 Products formed upon photolysis of octa acid encapsulated α-alkyldibenzyl ketones in borate buffer.[a]

Guest α-alkyl DBK	Type I products					Type II products		Type I: Type II products
	AA (**8**)	AB (**3**)	BB (**7**)	(**9**)	(**10**)	DBK (**12**)	CB (**11**)	
2a	–	75	–	4	21	–	–	–
2b	7	51	8	5	29	–	–	–
2c	–	50	–	4	35	4	7	89:11
2d	0	29	0	28	36	2	5	93:7
2e	0	28	0	34	32	3	3	94:6
2f	0	73	0	0	0	25	2	73:27
2 g	0	60	0	0	0	32	8	60:40
2 h	0	10	0	0	0	83	7	10:90

[a]Structures of, **2, 3**, **7**—**12**, DBK, and CB are included in Scheme 1. The data taken from Ref. 32

(**2f**, **2 g,** and **2 h**). The applicability of MD simulated structures in rationalizing the ketones dependent photoproducts distribution is addressed in the current study. It is important to note that in solution in the absence of a capsule all ketones behave in a similar manner (Table 1).

In this section, the process to determine the preferred structures of the guest DBK **2a – h** within the OA capsule is discussed. To keep the presentation concise, only one molecule from each group (**2a**, **2e,** and **2 g**) is chosen and the results of the rest are summarized in Supplementary Information (SI) section. During docking analysis, two conformers termed as "π–π" and "extended" for **2a** and "distorted" and "extended" for both **2e** and **2 g** were identified (Fig. 3, 4, and 5). The RMSD plots for both conformers of **2a** revealed a fast conversion of the π–π to the extended form. The latter form remained unchanged rest of the simulation time (100ns). To confirm the stability of this conformation, the simulation for the π–π form was further extended to 200 ns, and another simulation was performed at a much higher temperature (500 K). Both these simulations generated the same extended conformation (Fig. 3). In contrast, conformers (distorted and extended) of **2e** and **2g** provided by the docking procedure remained mostly unchanged throughout the simulations (Figs. 4 and 5). The stability of the structures over the extended simulation suggested that these are the preferred conformations of these molecules within the OA capsule.

Based on three parameters, binding energy, single point energy (Table 3), and the RMSD graph, the preferred structure of the ketones within the OA capsule is identified and are displayed in Fig. 6. It is clear that not all ketones prefer the same structure. To reiterate, the absolute value of binding energies presented in the table are not meaningful, but the difference in their values for two conformers helps to identify the most plausible binding mode of a guest inside the cavity of OA. Less preferred alternate MD representative structures for OA encapsulated **2c – 2 g** are shown in the Supplementary materials section (Fig. S3). These structures flipped to the more stable one with time as shown in Fig. S4 – S9 in the Supplementary Information section. Once again, based on the preferred structures the eight ketones can be classified into three groups: (1) **2a** and **2b**; (2) **2c**, **2d,** and **2e**, and (3) **2f**, **2 g**, **2 h**. This grouping has similarities, except for **2c**, to the classification made above based on their reactivities and ^{1}H NMR based structures. To get an insight into the phototransformations of **2a – h** to rearranged ketones **9** and **10** within the OA capsule, the encapsulation of **9c – h** and **10c – h** was investigated. The most favored structures obtained from MD simulations are shown in Figs. 7 and 8. In the next section, these structures are utilized to elucidate the interactions of the OA encapsulated ketones **2a – h** at the atomic level. Our goal is not to reinterpret the reactivities of the ketones **2a – h** based on structures presented in Fig. 6. It is mostly related to validate the applicability of MD simulations in providing structures that are consistent with the NMR spectral analyses.

4 Discussion

The OA capsule has been known to alter the excited state reactivity of a number of organic molecules [72–76]. Amongst these, its control on the photochemical behavior of alkyl substituted dibenzylketones undergoing competing reactions provides insight into the influence of confinement on excited state behavior of molecules enclosed in small spaces [32, 77, 78]. The importance of dibenzylketones as photochemical probes for confined and organized spaces (*eg*., micelles, zeolites etc.) was initially established by Turro [79–82]. In the current study, α-alkyldibenzylketones, a variation of dibenzylketone that undergo competing α-cleavage (Norrish type I) and γ-hydrogen abstraction (Norrish type II) reactions from their excited triplet states yielding multiple products (**3 – 13**, Scheme 1) are used as probes to understand the confining features of the OA capsule [32]. As shown

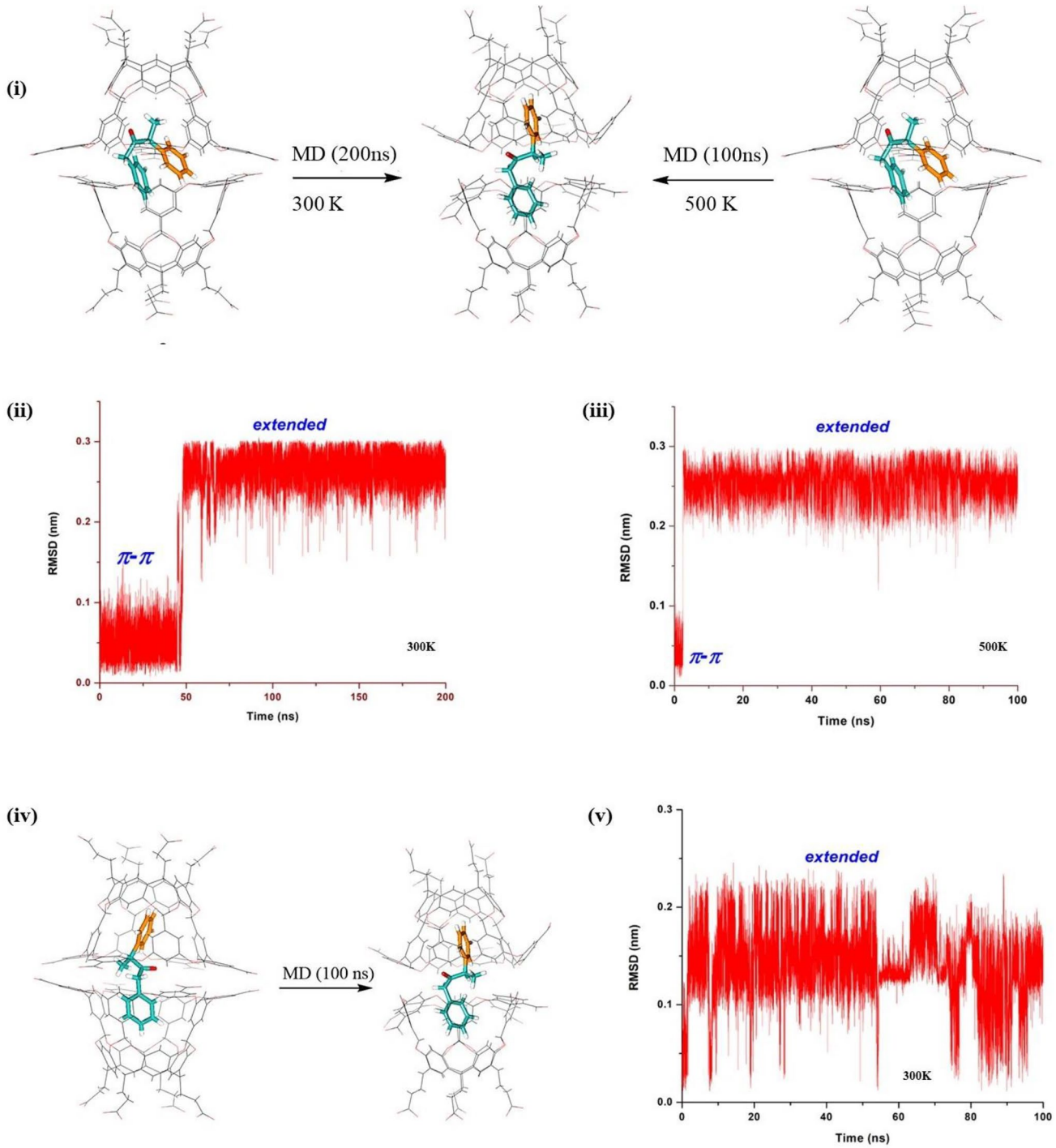

Fig. 3 i) Structures from the MD simulations of **2a** (π − π form), for 200ns at 300K and 100ns at 500K, ii) The root-mean-square-deviation (RMSD) of **2a** (guest only) trajectories calculated from the 200ns MD simulation at 300K, iii) The RMSD of **2a** at 500K from the 100ns MD trajectories, iv), The MD simulation of **2a** (extended form) for 100ns, and v) The RMSD of **2a** (extended form) at 300K

in Scheme 1, these molecules undergo α-cleavage to yield intermediates RP-1 and RP-2 (RP = radical pair). In isotropic solution, in the absence of confinement, RP-1 and RP-2 eliminate CO to give RP-5 which leads to the coupling products of A and B radicals in statistical amounts (AA: AB: BB, 1:2:1). When the alkyl chain contains γ-hydrogens, the γ-hydrogen abstraction by the excited carbonyl chromophore competes with the type I

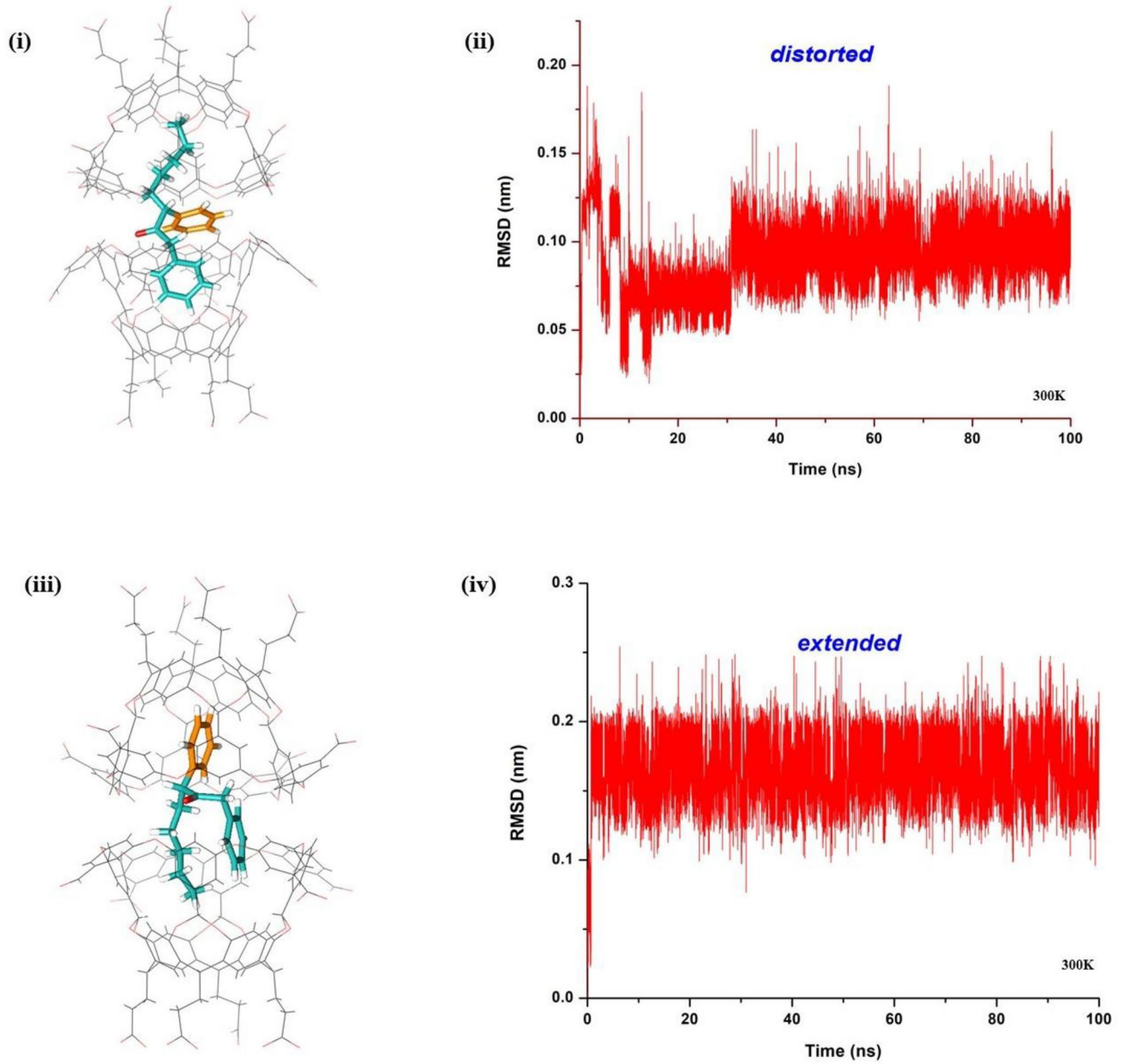

Fig. 4 i) The MD representative structure of **2e** (distorted π−π form), ii) The root-mean-square-deviation (RMSD) of **2e** (guest only, distorted π−π form) trajectories calculated from the 100ns MD simulation, iii) The MD representative structure of **2e** (extended form), and iv) The RMSD of **2e** (extended form) from the 100ns MD simulation

α-cleavage process. The 1,4-diradical intermediate formed via γ-hydrogen abstraction yields cyclization product **11** (Yang cyclization)[83] and fragmentation products **12** and **13**. From Table 1, it is clear that in hexane the products distribution is independent of the alkyl chain. Since the conformational freedom of the excited molecule is not restricted in isotropic solution, the alkyl chains even if it is present in a different conformation in the ground state, upon excitation can adopt the required conformation for hydrogen abstraction. Thus, in solution new electronic configuration is able to control the nuclear configuration and the medium is unable to resist the process. This, as noted in Table 1, results in the same ratio of type I and type II products for all ketones.

When the medium is rigid the reacting molecule and the intermediates would have very little mobility and upon excitation would be forced to yield products from structures/conformations that are close to the ground state one. For example, when RP-1 and RP-2 are confined they may undergo rearrangement to yield products **9** and **10** before

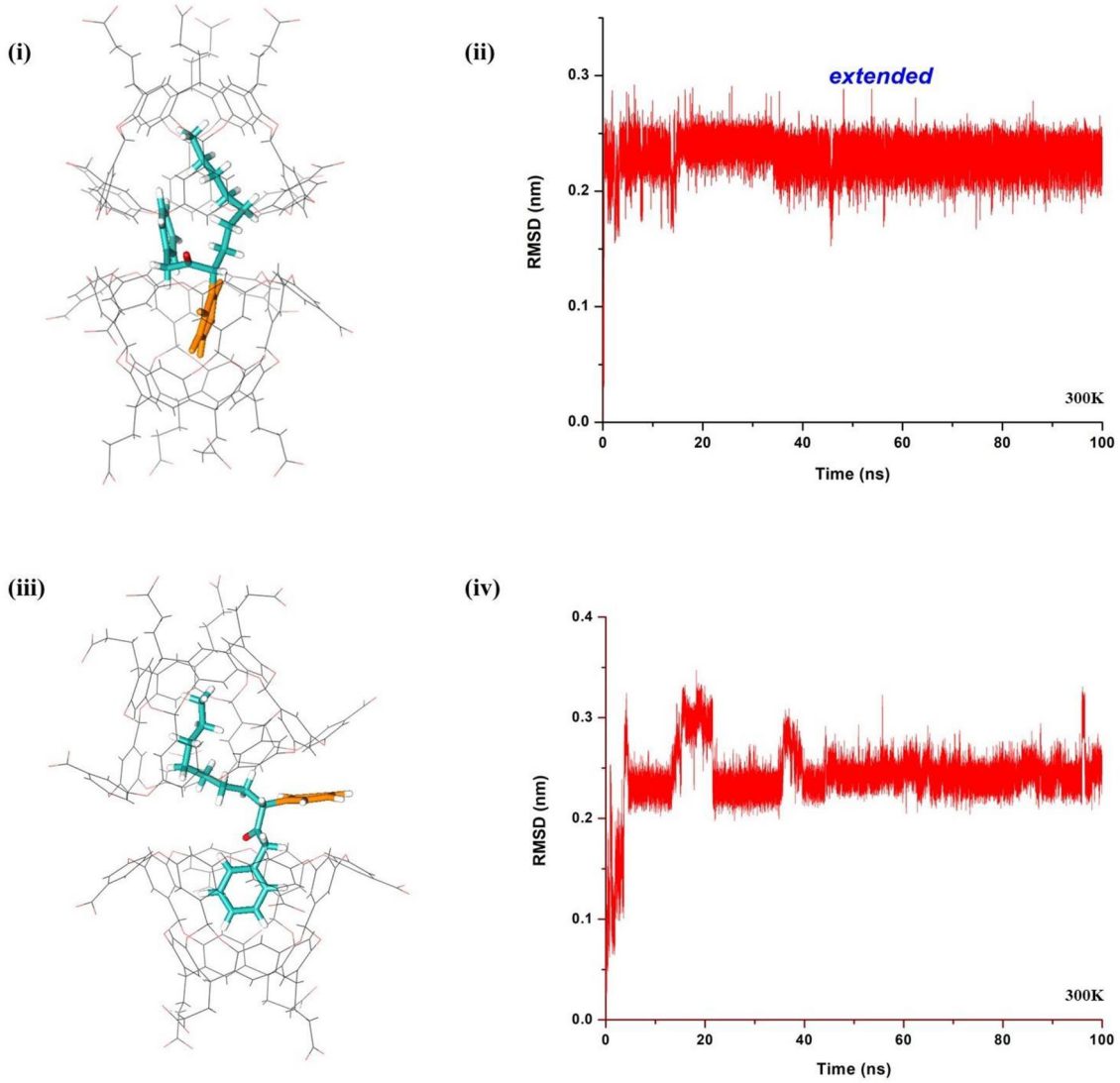

Fig. 5 i) The MD representative structure of **2g** (extended form), ii) The root-mean-square- deviation (RMSD) of **2g** (guest only, extended form) trajectories calculated from the 100ns MD simulation, iii) The MD representative structure of **2g**, and iv) The RMSD of **2g** from the 100ns MD simulation

they decarbonylate to give RP-5 (Scheme 1). Again, if RP-5 is confined, it would be forced to yield AB (**3**) and its rearrangement products (**4 – 6**) rather than AA and BB. Thus, the amounts of **9**, and **10,** and the coupling products of radicals A and B formed would depend on the extent of confinement and the freedom available for the intermediates. Further, since the γ-hydrogen abstraction is in competition with the α-cleavage, the conformational flexibility of the alkyl chain will determine the partition of the excited state between Norrish type I and type II pathways. Importantly, the extent of restriction of translational, rotational and conformational mobilities of the excited reactant and reactive intermediates is expected to depend on the free space within the reaction cavity and the rigidity of the cavity wall. Although products distributions in hexane are independent of the reacting molecules (Table 1), within the OA capsule they are dependent on the alkyl chain length (Table 2). To understand the chain length dependent products distributions within the OA capsule, we need to know the conformation of the ketones within the capsule and the free space around the reactant. Furthermore, to predict the feasibility of the γ-hydrogen abstraction, the interatomic distance between the carbonyl oxygen and γ-hydrogen should be known. Earlier we rationalized the products distributions listed in Table 2 based on guest conformation within the OA capsule derived from NMR spectra. Our goal is to establish that MD simulations of the host–guest structures (DBK**2a – h**@OA_2) can provide the required information to understand the unique

Table 3 Binding and single point energies for all MD simulated A-DBKs conformations in OA

OA capsular complexes	Binding energy (kcal/mol)	Single point energy [a] (E)	(ΔE, kcal/mol)[b]	Remarks
2a@OA_2 (π − π)	− 45.8	− 12,896.7244192	+ 22.3	Converts into extended
2a@OA_2 (extended)	− 47.2	− 12,896.7599425	0	
2b@OA_2 (π − π)	− 48.3	− 12,936.0783193	+ 16.1	
2b@OA_2 (distorted π − π)	− 49.6	− 12,936.0823075	+ 13.6	Converts into extended
2b@OA_2(extended)	− 50.4	− 12,936.1040438	0	
2c@OA_2 (distorted π − π)	− 53.3	− 12,975.4310467	0	
2c@OA_2 (extended)	− 51.0	− 12,975.3885317	+ 25.6	
2d@OA_2(distorted π − π)	− 57.5	− 13,014.5466799	0	Stable
2d@OA_2(extended)	− 57.8	− 13,014.5275863	+ 8.2	Unstable at 500 K
2e@OA_2 (distorted π − π)	− 57.4	− 13,054.0957151	0	
2e@OA_2 (extended)	− 55.4	− 13,054.0722112	+ 14.7	
2f@OA_2(extended)	− 69.6	− 13,086.8150378	0	
2f@OA_2(distorted π − π)	− 61.4	− 13,086.7815064	+ 21.0	
2 g@OA_2(extended)	− 64.9	− 13,126.1908252	0	
2 g@OA_2(distorted π − π)	− 69.2	− 13,126.1613809	+ 18.5	Capsule unstable
2 h@OA_2	− 63.4	− 13,165.5093039	–	Capsule is fully occupied

[a]The energy of MD simulated **2a − h**@OA_2 complex. Calculated using B3LYP hybrid functional and 6 − 31 + g(d) basis sets

[b]The difference of single point energy (ΔE) between isomers. The value '**0**' represents the isomer with lower energy and w.r.t that other isomer is shown in + **E** (higher in energy)

behavior of α-alkyldibenzylketones within the OA capsule. An excellent agreement with the measured NMR data for DBK**2a − h**@OA_2 makes a strong case to use this set of molecules as a probe to check the validity of MD simulations as a useful tool in supramolecular photochemistry.

Recognizing the lack of freedom for molecules and intermediates in crystals, Schmidt and his co-workers formulated the 'topochemical postulate' that states that reactions in the excited state occurs with very little motion in the crystalline state [9, 12–14]. Schmidt's group employed the crystal structures of molecules in the ground state to predict the chemical behavior in the excited state. The topochemical postulate continue to be the fundamental guiding principle for solid state photoreactions [84]. [85, 86] We believe that topochemical principles are applicable within any reaction cavity where the molecular freedom is restricted, and the medium is rigid [7, 8]. We demonstrate here that valuable insights could be gained into the reactivities of DBK **2a − h** from their MD simulated ground state structures shown in Fig. 6. Perusal of Table 2 reveals that the photochemical behavior of ketones **2a − h** investigated here can be classified into three groups: (a) the ones that give mainly AB (**3**) and its isomers (**4 − 6**) and the rearranged ketone **10**; (b) the ones that form AB and its isomers (**4 − 6**) and both rearranged ketones **9** and **10** and (c) the ones that provide products of γ-hydrogen abstraction and AB and yield no rearranged ketones. It is important to note the products in hexane are nearly the same for all **2a − h** ketones (Table 1). As will be discussed below that the MD equilibrated ground state structures (conformations) of **2a − h** within the confined space of the OA capsule rationalize the alkyl chain dependent photochemical behaviors of **2a − h** (Fig. 6).

Regarding type II reaction, ketones **2a** and **2b** do not possess γ-hydrogen and therefore no type II products are formed. On the other hand, ketones **2c**-**h** that possess γ-hydrogen yield products of type II. The product formation is independent of the alkyl chain length (~ 15%) in solution, while it depends on the length within the OA capsule (Table 2). In fact, for ketones **2f-h** the Type II products yields are 27, 40, and 90%, respectively. The MD equilibrated structures of the reactants (Fig. 6) shed light on these intriguing results. Evidently, conformations adopted by ketones **2f − h** within the OA capsule are distinctly different from that of all other ketones. In the thermodynamically most stable conformations of these molecules, the carbonyl group is oriented towards the γ-hydrogen favoring the abstraction. In addition, the distance between the γ-hydrogen and the carbonyl oxygen is estimated to be 3.2 Å or less than that (Table 4). (The distance distribution plot between γ-H and carbonyl O atom calculated along MD trajectories are provided in Fig S10 in the Supplementary section.) Scheffer et al. reported earlier that for type II reaction to occur in crystals the γ-hydrogen should be within 3.2 Å [87]. It is interesting to note that similar distance requirements are applicable even within the confined capsule of OA. As expected, when the distance is > 4 Å the contribution of type II reaction is minor within

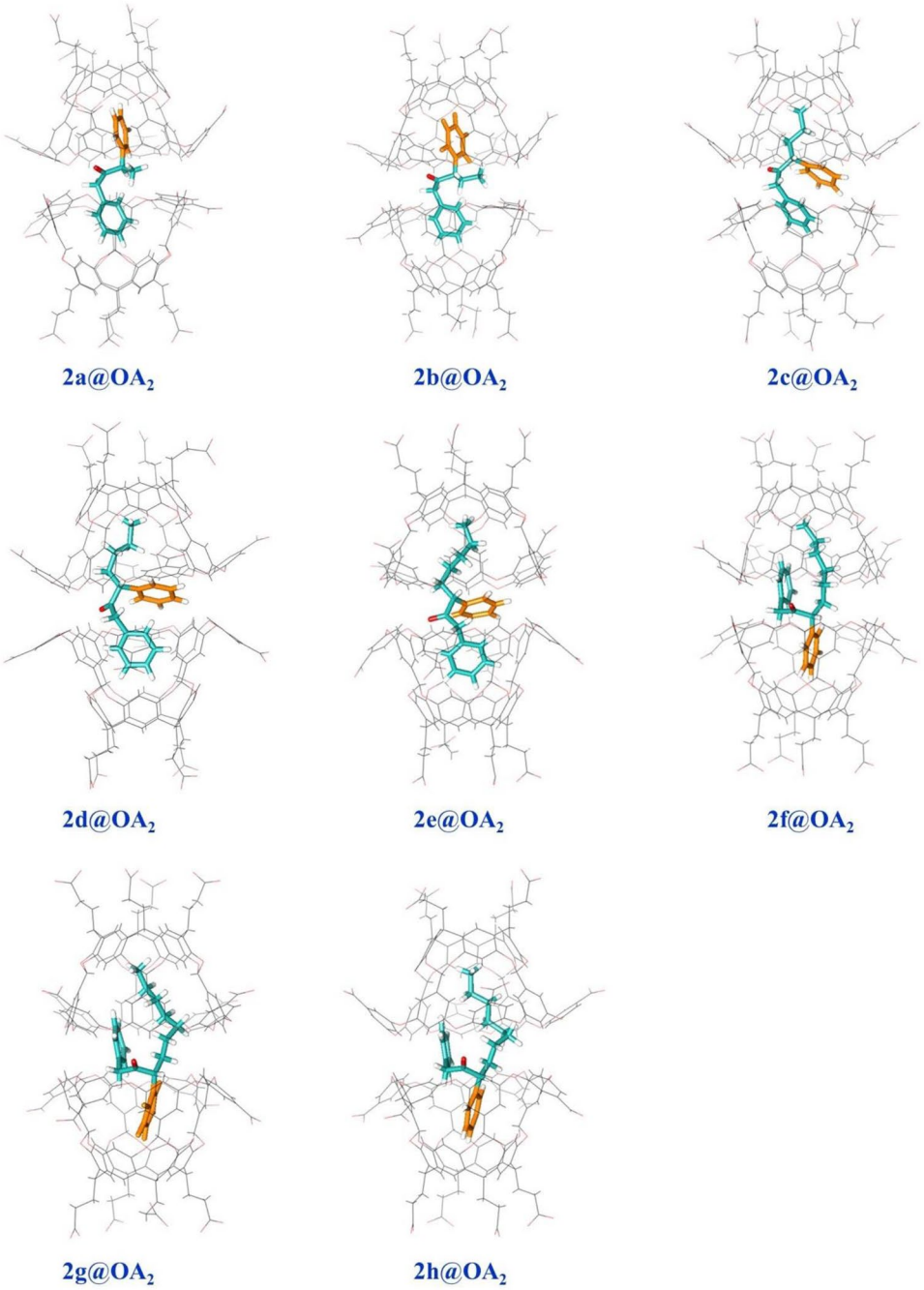

Fig. 6 The most representative structures (g-clustered) of **2a – h**@OA_2

the capsule (ketones **2c – e**; Table 2). One might argue that MD simulated structures are no different from the ones derived from NMR spectra. Because our goal is to test MD simulations as an alternative tool to obtain the same information, these results are valuable.

The next observation that needs to be understood is the absence of rearrangement products **9** and **10** from ketones **2f – h,** while **2a – e** give either both or single rearrangement product(s). Transformation of **2f – h** to **9** and **10** requires considerable free space within the OA capsule (Fig. 7). As seen in Table 4, the estimated free volumes within the OA capsule following the guest occupation are the smallest (229.7, 228.2 and 224.2 $Å^3$) for **2f – h** in the series. Rebek et al. reported that in guest – host complexes one could expect a maximum guest occupancy of 55% [88]. In these ketones, the occupancy level is > 60%. Under this condition, the guest molecules would be expected to have a very little free space to reorient. Thus, the absence of **9 a**nd **10** is consistent with the MD equilibrated structures of OA confined **2f – h** ketones. Finally, the increased contribution of Type II along the series **2h** > **2g** > **2f** is also in agreement with the decreased C = O–-γ–H distance, 2.8 < 3.0 < 3.2 Å

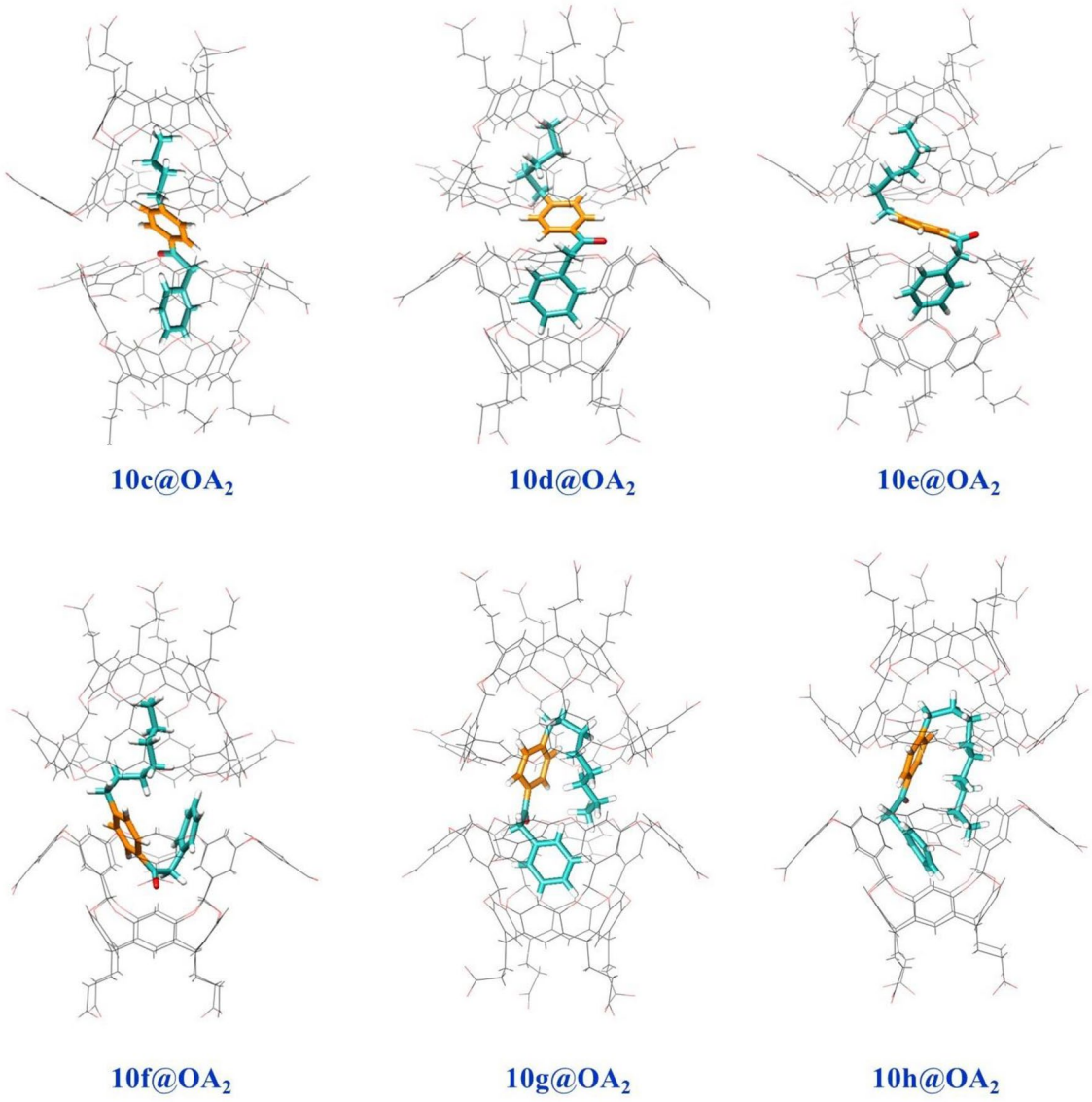

Fig. 7 The most representative structures (g-clustered) of photoproducts **10c – 10h**

(Table 4). Clearly, despite lacking electronic effects the MD simulated structures account for the excited state behavior of OA confined **2f – h** ketones. These agreements between the measured and computational results suggest that MD simulations can be a valuable tool to understand and predict chemical outcome in confined spaces.

As seen in Table 2, ketones **2a – c** inside the OA capsule mainly yield the rearranged ketone **10** and **AB** derived products from Norrish type I reaction; type II contribution is either zero or minimum. Absence of **BB** and **AA** and exclusive formation of **AB** have previously been understood on the basis of the 'cage effect', a concept that is widely discussed in the literature [89, 90]. Preference for the formation of **10** at the expense of **9** can be understood on the basis of the stability of the radical pair formed upon type I cleavage. In principle, upon excitation **2a – c** can cleave on either side of the carbonyl chromophore. Based on the stability of the resulting radical pair RP-1 *vs* RP-2, one would expect the more stable alkyl substituted radical pair RP-2 to be formed faster. This would lead to the rearranged product **10** via RP-4 provided there is enough space for it to rotate (Scheme 1). To examine the feasibility of rotation and availability of free space, as an illustrative example, MD simulations of **9** and **10** from **2c** within the OA capsule were performed. As seen in Figs. 7 and 8 the products **9** and **10** fit within the capsule. In ketones **2a – c**, the capsule permits the formation of both **9** and **10**. As shown in Table 4, the capsule has plenty of free space following the occupancy of the reactant ketones (292–302 $Å^3$), the most in the series. Also, the capsular occupancy is less than 50%, much less than when the

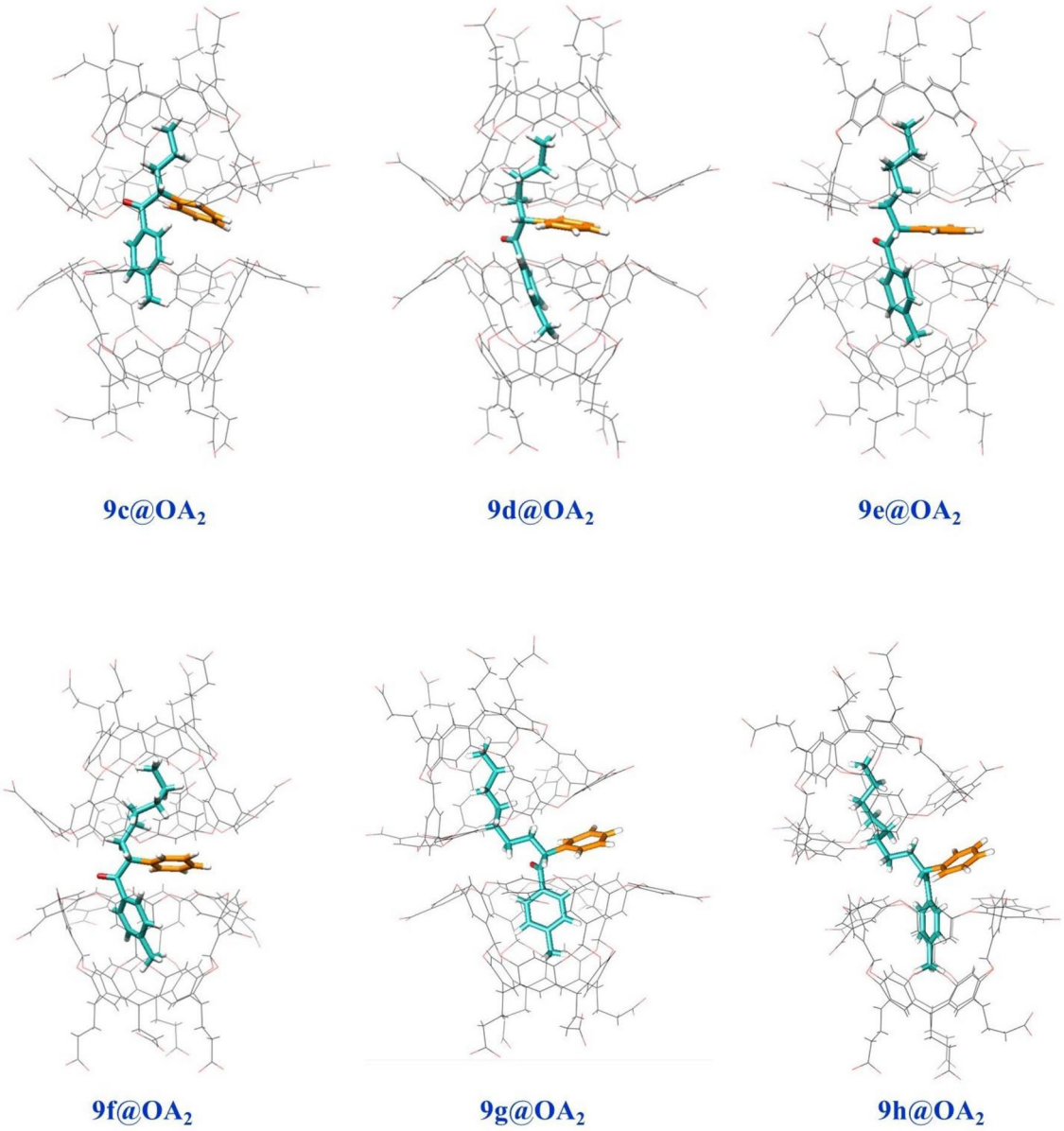

Fig. 8 The most representative structures (g-clustered) of photoproducts **9c – 9h**

capsule is occupied by **2f – h**. The preference for **10** arises at the early stage of cleavage where the stability of the radical pair drives the reaction towards RP-2. Thus, the principles of physical organic chemistry (stability of the radical pair), supramolecular chemistry (cage effect) and results of MD simulations (identification of free space) aid in understanding the unique behavior of the ketones **2a – c** within the capsule.

The final observation that needs to be understood deals with the behavior of **2d** and **e**. These two ketones, once again behave differently from the remaining six. In these cases, once again Norrish type I is the predominant reaction. However, unlike **2a – c**, they yield both rearranged ketones **9** and **10**. Based on the stability of the resulting radicals, one would expect the formation of RP-2 to dominate over RP-1. Why would a product (**9**) from less likely α-cleavage process (to yield RP-1) will form? Once again, the answer is found in the MD equilibrated structures of the complexes (Fig. 6). In cases where rotation of RP-2 to form RP-4 is slowed by the confinement, the slow path of via the RP-1 and RP-3 to **9** would be able to compete with the formation of **10**. The selection of a pathway can be explained on the basis of the available free volume within the capsule (Table 4). Interestingly, the free space in the case of **2d** and **2e** is larger than that for **2f – h**. In the latter case with much less free space (< 230 Å^3) there are no rearrangement products. Probably,

Table 4 Percentage occupancy, free space, and γ − H distance of DBK within octa acid (OA)

Host − guest complexes	Volume (Å^3)	Guest	Volume of guest (Å^3)	% Occupancy of the reaction cavity	Free space within the reaction cavity[d] (Å^3)	γ − H distance[e] (Å)
2a@OA_2	522.7[a]	**2a**	230.3	44[b] (43.4)[c]	292.4	–
2b@OA_2	554.9[a]	**2b**	252.7	46[b] (47.6)[c]	302.2	5.2
2c@OA_2	566.3[a]	**2c**	269.5	48[b] (50.8)[c]	296.8	4.6
2d@OA_2	540.9[a]	**2d**	286.9	53[b] (54.0)[c]	254.0	4.8
2e@OA_2	549.2[a]	**2e**	302.5	55[b] (57.0)[c]	246.7	4.5
2f@OA_2	549.3[a]	**2f**	319.6	58[b] (60.2)[c]	229.7	3.2
2 g@OA_2	564.3[a]	**2 g**	336.1	60[b] (63.3)[c]	228.2	3.0
2 h@OA_2	577.2[a]	**2 h**	353.0	61[b] (66.5)[c]	224.2	2.8

[a]Volume of OA cavity after removing A-DBK from the complex. This gives the idea of change in volume of capsular cavity in presence of different guests

[b]The ratio of A-DBKs volume over cavity volume (OA)

[c]The ratio of A-DBKs volume over standard cavity volume (standard OA, volume 533.9 Å^3)

[d]The free space is the difference between cavity volume (OA) and guest's volume

[e]The average distance between γ-hydrogen and oxygen atom. Calculated using VMD (virtual molecular dynamics)

slightly larger free volume in the case of **2d** and **2e** (254 and 246 Å^3; Table 4) with respect to **2f − h** does not fully inhibit the tumbling within the capsule but makes it a slow process. Apparently, slightly smaller free volume with respect to **2a − c** (> 290Å^3, Table 4) makes the rotation slow. Most likely, slowing of the tumbling of RP-2 is also a result of the location and conformation of the alkyl chain within the capsule (Fig. 6). Rearrangement of **2d** and **2e** to **10** would require the chain to further penetrate the capsule when there is no room available (Fig. 7). Thus, by examining the structures of the reactant ketone and the product **10** (Figs. 6 and 7) one could conclude that the pathway leading to **10** in the case of ketones **2d** and **2e** would be slow. On the other hand, conversion of **2d** and **2e** to **9** would not be inhibited within the capsule (Fig. 8). Although the rate of initial cleavage is expected to be slow, this pathway could eventually win because the later step is slowed down by the capsule for the formation of **10**. It is important to recognize that these conclusions could not have been drawn without knowing the structure of host − guest complexes.

5 Conclusion

To conclude, we have rationalized the alkyl chain length dependent photoreactivity of a series of related α-alkyl dibenzylketones encapsulated within the OA capsule based on MD simulated structures of the host (OA) − guest complexes. Clearly the ground state conformation and structure of encapsulated ketones are to a large extent retained even in the excited state because of the restriction provided by the 'hard and inflexible' reaction cavity of the OA capsule [7, 8]. Since the reactions occur within a rigid small space, the cavity characteristics also play a role. From the MD simulated structures of the host − guest complexes, we have been able to identify the extent of free space available within the OA capsule. This information is valuable in predicting the behavior of confined α-alkyl dibenzylketones. Further, the feasibility of type II hydrogen abstraction in some ketones is revealed by the distance between the reactive carbonyl oxygen and γ-hydrogen. In our earlier publication, we had used the information obtained from 1 and 2D ^{1}H NMR spectroscopy to identify the structure of host − guest complexes and to rationalize structure − reactivity relationship within the OA capsule. Such spectra provided information only about the guest structure independent of the host. Intracavity relationships between the guest and the host are not readily obtained by the above experimental approach. Also, information regarding the cavity free space and inter-atomic distances could only be extracted from MD simulated structures.

As mentioned above, there are limitations for the approach adopted in this study since the simulations do not consider electronic configurations of the reactant molecule. When the space is limited, it is known that the environment plays a major role in controlling the dynamics of a molecule rather than the new electronic configuration reached upon light absorption. Results presented above with well investigated ketones included in a rigid capsule suggest that the MD simulations can be a valuable tool in understanding excited state chemistry in rigid environments. Ideally to quantitatively interpret photoreactions in supramolecular assemblies one should employ hybrid quantum mechanics/molecular mechanics (QM/MM) methods. We have recently reported the excited state chemistry of anthracene within the OA capsule where such an approach was employed [33]. In the future, this may become the method of choice, especially with the groups with considerable resources and expertise.

Given the time and resource demand at this time not everyone can afford to employ such a sophisticated approach. Under such conditions, a simpler approach described here is useful to qualitatively assess the trend in reactivity of structurally related molecules. Results discussed here illustrate MD simulations that is accessible to nonexperts could be useful in understanding excited state reactions in confined spaces. More importantly, the message that comes out of this study is that when the molecule is confined, the electronic configuration in the excited state and nuclear configuration in the ground state play roles in the dynamics of molecules on the excited state surface. On the other hand, in isotropic solution where the medium is soft and flexible the nuclear configuration controlled by the excited state electronic configuration dominates the chemistry. This difference makes the supramolecular photochemistry in rigid environments distinctly different from molecular photochemistry and the search for new reactions by confining molecules rewarding. Identifying conical intersections on excited state surfaces of these confined molecules is expected to be challenging and in all probability, these would be at a different place from that for free molecules [34]. Pursuit of such studies is beyond our reach at this stage but we are optimistic this would interest others in the future.

Supplementary Information The online version contains supplementary material available at https://doi.org/10.1007/s43630-023-00486-2.

Acknowledgements The authors thank the National Science Foundation (VR: CHE-2204046 and RP: CHE-2102563) for financial support. Computational resources from the University of Miami Institute for Data Science and Computing (IDSC) are greatly acknowledged.

Data availability Data will be available on request.

Declarations

Conflict of interest There are no conflicts of interest to declare.

References

1. Turro, N. J., Ramamurthy, V., & Scaiano, J. C. (2010). *Modern molecular photochemistry of organic molecules*. University Science Books.
2. Klan, P., & Wirz, J. (2009). *Photochemistry of organic compounds*. John Wiley & Sons Ltd.
3. Photochemistry in Organized and Constrained Media, V. Ramamurthy (Ed.), VCH Publishers, New York, 1991.
4. Supramolecular Photochemistry, V. Ramamurthy & Y. Inoue (Eds.), John Wiley, Hoboken, 2011.
5. Supramolecular Photochemistry, V. Balzani & F. Scandola (Eds.), Ellis Horwood, Chichester, UK, 1991.
6. Frontiers in Supramolecular Organic Chemistry and Photochemistry, H.-J. Schneider & H. Durr (Eds.),VCH, New York, 1991.
7. V. Ramamurthy, R.G. Weiss & G.S. Hammond, A Model for the Influence of Organized Media on Photochemical Reactions, Advances in Photochemistry, Vol. 18, John Wiley & Sons, Inc., **1993**. pp. 67–234.
8. Weiss, R. G., Ramamurthy, V., & Hammond, G. S. (1993). Photochemistry in organized and confining media: a model. *Accounts of Chemical Research, 26*, 530–536.
9. G.M.J. Schmidt,The photochemistry of the solid state, Reactivity of the photoexcited organic molecule, Proceedings of the Thirteenth Conference on Chemistry at the University of Brussels, October 1965, John Wiley, New York, 1967, 227–288.
10. Ramamurthy, V., & Sivaguru, J. (2016). Supramolecular photochemistry as a synthetic tool: photocycloaddition. *Chemical Reviews, 116*, 9914–9993.
11. Ramamurthy, V., & Venkatesan, K. (1987). Photochemical reactions of organic crystals. *Chemical Reviews, 87*, 433–481.
12. G. M. J. Schmidt et al. Solid State Photochemistry, D. Ginsburg ((Ed.), Verlag Chemie, Weinheim, 1976.
13. Cohen, M. D. (1975). The photochemistry of organic solids. *Angewandte Chemie (International ed. in English), 14*, 386–393.
14. G.M.J. Schmidt, (1964), Topochemistry. III. The crystal chemistry of some trans-cinnamic acids, *J. Chem. Soc.*, 2014–2021.
15. Gibb, C. L. D., & Gibb, B. C. (2004). Well-defined, organic nanoenvironments in water: the hydrophobic effect drives capsular assembly. *Journal of the American Chemical Society, 126*, 11408–11409.
16. Choudhury, R., Barman, A., Prabhakar, R., & Ramamurthy, V. (2013). Hydrocarbons depending on the chain length and head group adopt different conformations within a water-soluble nanocapsule: ^{1}H NMR and molecular dynamics studies. *The Journal of Physical Chemistry B, 117*, 398–407.
17. Kulasekharan, R., Choudhury, R., Prabhakara, R., & Ramamurthy, V. (2011). Restricted rotation due to the lack of free space within a capsule translates into product selectivity: Photochemistry of cyclohexyl phenyl ketones within a water-soluble organic capsule. *Chemical Communications, 47*, 2841–2843.
18. Ramkumar Varadharajan, Sarah Ariel Kelley, Vindi M. Jayasinghe-Arachchige, Rajeev Prabhakar, V. Ramamurthy & S.C. Blackstock, (2022), Organic Host Encapsulation Effects on Nitrosobenzene Monomer−Dimer Distribution and C−NO Bond Rotation in an Aqueous Solution, *ACS Org. Inorg. Au*, *2*, 175-185
19. A.H. Elcock, D. Sept & J.A. McCammon, (2001), Computer Simulation of Protein−Protein Interactions, *J. Phys. Chem., B*, *105*, 1504–1518.
20. Baaden, M., & Marrink, S. J. (2013). Coarse-grain modelling of protein–protein interactions. *Current Opinion in Structural Biology, 23*, 878–886.
21. Basdevant, N., Weinstein, H., & Ceruso, M. (2006). Thermodynamic basis for promiscuity and selectivity in protein−protein interactions: PDZ domains, a case study. *Journal of the American Chemical Society, 128*, 12766–12777.
22. Salsbury, F. R. (2010). Molecular dynamics simulations of protein dynamics and their relevance to drug discovery. *Current Opinion in Pharmacology, 10*, 738–744.
23. Friedman, R. (2022). Computational studies of protein–drug binding affinity changes upon mutations in the drug target. *WIREs Computational Molecular Science, 12*, e1563.
24. Ozbil, M., Barman, A., Bora, R. P., & Prabhakar, R. (2012). Computational insights into dynamics of protein aggregation and enzyme-substrate interactions. *J. Pjys. Chem. Lett., 3*, 3460–3469.
25. Díaz, N., Sordo, T. L., Merz, K. M., & Suárez, D. (2003). Insights into the acylation mechanism of class A β-lactamases from molecular dynamics simulations of the TEM-1 enzyme complexed with benzylpenicillin. *Journal of the American Chemical Society, 125*, 672–684.
26. Sharma, G., Hu, Q., Jayasinghe-Arachchige, V. M., Paul, T. J., Schenk, G., & Prabhakar, R. (2019). Investigating coordination flexibility of glycerophosphodiesterase (GpdQ) through interactions with mono-, di-, and triphosphoester (NPP, BNPP, GPE,

and paraoxon) substrates. *Physical Chemistry Chemical Physics: PCCP, 21*, 5499–5509.
27. Cisneros, G. A., Karttunen, M., Ren, P., & Sagui, C. (2014). Classical electrostatics for biomolecular simulations. *Chemical Reviews, 114*, 779–814.
28. R. Kapral & G. Ciccotti,Chapter 16 - Molecular dynamics: An account of its evolution, C.E. Dykstra, G. Frenking, K.S. Kim, G.E. Scuseria (Eds.) Theory and Applications of Computational Chemistry, Elsevier, Amsterdam, 2005, 425–441.
29. Rahman, A., & Stillinger, F. H. (2003). Molecular dynamics study of liquid water. *The Journal of Chemical Physics, 55*, 3336–3359.
30. H.J.C. Berendsen, Molecular dynamics simulations: The limits and beyond, Springer, 1999.
31. Pokorna, P., Kruse, H., Krepl, M., & Sponer, J. (2018). QM/MM calculations on protein–RNA complexes: Understanding limitations of classical MD simulations and search for reliable cost-effective QM methods. *Journal of Chemical Theory and Computation, 14*, 5419–5433.
32. Gibb, C. L. D., Sundaresan, A. K., Ramamurthy, V., & Gibb, B. C. (2008). Templation of the excited-state chemistry of α-(n-Alkyl) Dibenzyl ketones: How guest packing within a nanoscale supramolecular capsule influences photochemistry. *Journal of the American Chemical Society, 130*, 4069–4080.
33. Das, A., Danao, A., Banerjee, S., Raj, A. M., Sharma, G., Prabhakar, R., Srinivasan, V., Ramamurthy, V., & Sen, P. (2021). Dynamics of anthracene excimer formation within a water-soluble nanocavity at room temperature. *Journal of the American Chemical Society, 143*, 2025–2036.
34. Boeije, Y., & Olivucci, M. (2023). From a one-mode to a multimode understanding of conical intersection mediated ultrafast organic photochemical reactions. *Chemical Society Reviews, 52*, 2643–2687.
35. Zhu, T., & Van Voorhis, T. (2016). Charge recombination in phosphorescent organic light-emitting diode host–guest systems through qm/mm simulations. *Journal of Physical Chemistry C, 120*, 19987–19994.
36. M. Olsson, A. & U. Ryde, (2017), Comparison of QM/MM Methods to Obtain Ligand-Binding Free Energies, *J. Chem. Theory Comput.*, *13*, 2245-2253
37. Wang, M., Mei, Y., & Ryde, U. (2019). Host–guest relative binding affinities at density-functional theory level from semiempirical molecular dynamics simulations. *Journal of Chemical Theory and Computation, 15*, 2659–2671.
38. Wang, M., Mei, Y., & Ryde, U. (2018). Predicting relative binding affinity using nonequilibrium QM/MM simulations. *Journal of Chemical Theory and Computation, 14*, 6613–6622.
39. Steinmann, C., Olsson, M. A., & Ryde, U. (2018). Relative ligand-binding free energies calculated from multiple short QM/MM MD simulations. *Journal of Chemical Theory and Computation, 14*, 3228–3237.
40. Caldararu, O., Olsson, M. A., Misini Ignjatović, M., Wang, M., & Ryde, U. (2018). Binding free energies in the SAMPL6 octa-acid host–guest challenge calculated with MM and QM methods. *Journal of Computer-Aided Molecular Design, 32*, 1027–1046.
41. Caldararu, O., Olsson, M. A., Riplinger, C., Neese, F., & Ryde, U. (2017). Binding free energies in the SAMPL5 octa-acid host–guest challenge calculated with DFT-D3 and CCSD (T). *Journal of Computer-Aided Molecular Design, 31*, 87–106.
42. Olsson, M. A., Söderhjelm, P., & Ryde, U. (2016). Converging ligand-binding free energies obtained with free-energy perturbations at the quantum mechanical level. *Journal of Computational Chemistry, 37*, 1589–1600.
43. Mikulskis, P., Cioloboc, D., Andrejić, M., Khare, S., Brorsson, J., Genheden, S., Mata, R. A., Söderhjelm, P., & Ryde, U. (2014). Free-energy perturbation and quantum mechanical study of SAMPL4 octa-acid host–guest binding energies. *Journal of Computer-Aided Molecular Design, 28*, 375–400.
44. Andrejić, M., Ryde, U., Mata, R. A., & Söderhjelm, P. (2014). Coupled-cluster interaction energies for 200-atom host-guest systems. *ChemPhysChem, 15*, 3270–3281.
45. Jing, Z., Liu, C., Cheng, S. Y., Qi, R., Walker, B. D., Piquemal, J.-P., & Ren, P. (2019). Polarizable force fields for biomolecular simulations: recent advances and applications. *Ann. Rev. Biophys., 48*, 371–394.
46. Nakata, H., & Bai, S. (2019). Development of a new parameter optimization scheme for a reactive force field based on a machine learning approach. *J. Comp. Chem., 40*, 2000–2012.
47. He, X., Man, V. H., Yang, W., Lee, T.-S., & Wang, J. (2020). A fast and high-quality charge model for the next generation general AMBER force field. *The Journal of Chemical Physics, 153*, 114502.
48. Grimme, S. (2019). Exploration of chemical compound, conformer, and reaction space with meta-dynamics simulations based on tight-binding quantum chemical calculations. *Journal of Chemical Theory and Computation, 15*, 2847–2862.
49. Kulasekharan, R., Choudhury, R., Prabhakar, R., & Ramamurthy, V. (2011). Restricted rotation due to the lack of free space within a capsule translates into product selectivity: Photochemistry of cyclohexyl phenyl ketones within a water-soluble organic capsule. *Chemical Communications, 47*, 2841–2843.
50. Becke, A. D. (1988). Density-functional exchange-energy approximation with correct asymptotic behavior. *J. Phys. Rev. A, 38*, 3098–3100.
51. A.D. Becke, Density-functional thermochemistry. III The role of exact exchange, *J. Chem. Phys.*, 1993.
52. Grimme, S., Ehrlich, S., & Goerigk, L. (2011). Effect of the damping function in dispersion corrected density functional theory. *J. Comp. Chem., 32*, 1456–1465.
53. M. Frisch, G.W. Trucks, H.B. Schlegel, G.E. Scuseria, M.A. Robb, J.R. Cheeseman, G. Scalmani, V. Barone, B. Mennucci & G. Petersson, Gaussian 09, revision D. 01, Gaussian, Inc., Wallingford CT, 2009.
54. Francl, M. M., Pietro, W. J., Hehre, W. J., Binkley, J. S., Gordon, M. S., DeFrees, D. J., & Pople, J. A. (1982). Self-consistent molecular orbital methods. XXIII. A polarization-type basis set for second-row elements. *The Journal of Chemical Physics, 77*, 3654–3665.
55. Rassolov, V. A., Ratner, M. A., Pople, J. A., & P.l.C. Redfern & L.A. Curtiss,. (2001). 6–31G* basis set for third-row atoms. *J. Comp. Chem., 22*, 976–984.
56. Mennucci, B. (2012). Polarizable continuum model. *WIREs Computational Molecular Science, 2*, 386–404.
57. Wang, J., Wolf, R. M., Caldwell, J. W., Kollman, P. A., & Case, D. A. (2004). Development and testing of a general amber force field. *J. Comp. Chem., 25*, 1157–1174.
58. Wang, J., Wang, W., Kollman, P. A., & Case, D. A. (2006). Automatic atom type and bond type perception in molecular mechanical calculations. *Journal of Molecular Graphics, 25*, 247–260.
59. Case, D. A., Cheatham Iii, T. E., Darden, T., Gohlke, H., Luo, R., Merz, K. M., Jr., Onufriev, A., Simmerling, C., Wang, B., & Woods, R. J. (2005). The Amber biomolecular simulation programs. *J. Comp. Chem., 26*, 1668–1688.
60. Trott, O., & Olson, A. J. (2010). AutoDock Vina: Improving the speed and accuracy of docking with a new scoring function, efficient optimization, and multithreading. *J. Comp. Chem., 31*, 455–461.
61. Hess, B., Kutzner, C., Van Der Spoel, D., & Lindahl, E. (2008). GROMACS 4: Algorithms for highly efficient, load-balanced, and scalable molecular simulation. *J. Chem. Theory., 4*, 435–447.
62. Pronk, S., Páll, S., Schulz, R., Larsson, P., Bjelkmar, P., Apostolov, R., Shirts, M. R., Smith, J. C., Kasson, P. M., & Van Der

Spoel, D. (2013). GROMACS 4.5: A high-throughput and highly parallel open source molecular simulation toolkit. *Bioinfo., 29*, 845–854.
63. Case, D. A., Cheatham, T. E., III., Darden, T., Gohlke, H., Luo, R., Merz, K. M., Jr., Onufriev, A., Simmerling, C., Wang, B., & Woods, R. J. (2005). The Amber biomolecular simulation programs. *Journal of Computational Chemistry, 26*, 1668–1688.
64. Price, D. J., & Brooks, C. L., III. (2004). A modified TIP3P water potential for simulation with Ewald summation. *The Journal of Chemical Physics, 121*, 10096–10103.
65. Hess, B., Bekker, H., Berendsen, H. J. C., & Fraaije, J. (1997). LINCS: A linear constraint solver for molecular simulations. *J. Comp. Chem., 18*, 1463–1472.
66. Miyamoto, S., & Kollman, P. A. (1992). Settle: An analytical version of the SHAKE and RATTLE algorithm for rigid water models. *J. Comp. Chem., 13*, 952–962.
67. Darden, T., York, D., & Pedersen, L. (1993). Particle mesh Ewald: An N· log (N) method for Ewald sums in large systems. *The Journal of Chemical Physics, 98*, 10089–10092.
68. Kollman, P. A., Massova, I., Reyes, C., Kuhn, B., Huo, S., Chong, L., Lee, M., Lee, T., Duan, Y., Wang, W., Donini, O., Cieplak, P., Srinivasan, J., Case, D. A., & Cheatham, T. E., III. (2000). Calculating structures and free energies of complex molecules: combining molecular mechanics and continuum models. *Accounts of Chemical Research, 33*, 889–897.
69. Humphrey, W., Dalke, A., & Schulten, K. (1996). VMD: Visual molecular dynamics. *Journal of Molecular Graphics, 14*, 33–38.
70. Krieger, E., & Vriend, G. (2002). Models@ Home: Distributed computing in bioinformatics using a screensaver based approach. *Bioinfo., 18*, 315–318.
71. Pettersen, E. F., Goddard, T. D., Huang, C. C., Couch, G. S., Greenblatt, D. M., Meng, E. C., & Ferrin, T. E. (2004). UCSF Chimera—a visualization system for exploratory research and analysis. *J. Comp. Chem., 25*, 1605–1612.
72. Ramamurthy, V. (2015). Photochemistry within a water-soluble organic capsule. *Accounts of Chemical Research, 48*, 2904–2917.
73. Ramamurthy, V., Jockusch, S., & Porel, M. (2015). Supramolecular photochemistry in solution and on surfaces: encapsulation and dynamics of guest molecules and communication between encapsulated and free molecules. *Langmuir, 31*, 5554–5570.
74. Das, A., Ghosh, S. K., Ramamurthy, V., & Sen, P. (2022). Vibration-assisted intersystem crossing in the ultrafast excited state relaxation dynamics of halocoumarins. *Journal of Physical Chemistry A, 126*, 1475–1485.
75. V. Ramamurthy,Controlling Excited State Chemistry of Organic Molecules in Water Through Incarceration, P.K. Chattaraj, D. Chakraborty (Eds.) Chemical Reactivity in Confined Systems: Theory, Modelling and Applications, John Wiley, Hoboken, NJ, 2021, 335–338.
76. Ramamurthy, V., Sen, P., & Elles, C. G. (2022). Ultrafast excited state dynamics of spatially confined organic molecules. *Journal of Physical Chemistry A, 126*, 4681–4699.
77. Sundaresan, A. K., & Ramamurthy, V. (2007). Making a difference on excited-state chemistry by controlling free space within a nanocapsule: photochemistry of 1-(4-Alkylphenyl)-3-phenylpropan-2-ones. *Organic Letters, 9*, 3575–3578.
78. Sundaresan, A. K., & Ramamurthy, V. (2008). Consequences of controlling free space within a reaction cavity with a remote alkyl group: Photochemistry of para-alkyl dibenzyl ketones within an organic capsule. *Photochemical & Photobiological Sciences, 7*, 1555–1564.
79. Turro, N. J., & Cherry, W. R. (1978). Photoreactions in detergent solutions. enhancement of regioselectivity resulting from the reduced dimensionality of substrates sequestered in a micelle. *Journal of the American Chemical Society, 100*, 7431–7432.
80. Turro, N. J., & Kraeutler, B. (1978). Magnetic Isotope and Magnetic Field Effects on Chemical Reactions. Sunlight and Soap for the Efficient Separation of ^{13}Cand ^{12}C Isotopes. *Journal of the American Chemical Society, 100*, 7432–7434.
81. Gould, I. R., Zimmt, M. B., Turro, N. J., Baretz, B. H., & Lehr, G. F. (1985). Dynamics of radical pair reactions in micelles. *Journal of the American Chemical Society, 107*, 4607–4612.
82. Turro, N. J. (2000). From boiling stones to smart crystals: supramolecular and magnetic isotope control of radical-radical reactions inside zeolites. *Accounts of Chemical Research, 33*, 637–646.
83. Yang, N. C., & Yang, D.-D.H. (1958). Photochemical reactions of ketones in solution. *Journal of the American Chemical Society, 80*, 2913–2914.
84. Scheffer, J. R. (2001). In the footsteps of Pasteur: Asymmetric induction in the photochemistry of crystalline ammonium carboxylate salts. *Canadian Journal of Chemistry, 79*, 349–357.
85. A.E. Keating & A. Garcia-Garibay Miguel,Photochemical Solid-to-Solid Reactions, V. Ramamurthy, K.S. Schanze (Eds.) Molecular and Supramolecular Photochemistry, Marcel Dekker, Inc., New York, 2002, 195.
86. K. Tanaka & F. Toda,Organic Photoreaction in the Solid State, F. Toda (Ed.) Organic Solid State Reactions, Kluwer Academic Publishers, Dordrecht, 2002, 109–158.
87. Ihmels, H., & Scheffer, J. R. (1999). The Norrish type II reaction in the crystalline state: Toward a better understanding of the geometric requirements for γ-hydrogen atom abstraction. *Tetrahedron, 55*, 885–907.
88. Mecozzi, S., & Julius Rebek, J. (1998). The 55% solution: a formula for molecular recognition in the liquid state. *Chemistry--A European Journal, 4*, 1016–1022.
89. Noyes, R. M. (1961). Effects of diffusion rates on chemical kinetics. *Prog. React. Kinetics, 1*, 131–160.
90. Turro, N. J., & Kraeutler, B. (1980). Magnetic field and magnetic isotope effects in organic photochemical reactions. a novel probe of reaction mechanisms and a method for enrichment of magnetic isotopes. *Accounts of Chemical Research, 13*, 369–377.

Authors and Affiliations

Dipendra Khadka[1] · Vindi M. Jayasinghe-Arachchige[1] · Rajeev Prabhakar[1] · Vaidhyanathan Ramamurthy[1]

✉ Rajeev Prabhakar
rpr@miami.edu

✉ Vaidhyanathan Ramamurthy
murthy1@miami.edu

[1] Department of Chemistry, University of Miami, Coral Gables, FL 33124, USA